Dieter Baldinger

Comparing the effects of morphological variation in locomotion using a salamander-like robot to salamanders locomotor system

Semester Thesis

Biorobotics Laboratory
École polytechnique fédérale de Lausanne (EPFL)

Supervision

Kostas Karakasiliotis
Prof. Auke Jan Ijspeert

June 2012

Preface

I would like to thank Professor Auke Jan Ijspeert for the opportunity to continue the work of the previous project in his lab. Many thanks to Konstantinos Karakasiliotis for the great support during the project. Constructive discussions helped me to understand difficult part and find a good strategy to pursue the goals. Furthermore, I want to thank Alessandro Crespi for his big patience and support for every hardware problem occurred during this project.

Contents

Nomenclature

Symbols

A	Amplitude	[°]
DF	Duty factor	[−]
f	Frequency	[Hz]
k	Number of waves	[−]
M	Morphology	[−]
α	Joint anlge	[°]
β	Body bending	[°]
ϕ	Phase lag	[−]
ψ	Offset	[°]

Indicies

aq	aquatic
te	terrestrial

Acronyms and Abbreviations

EPFL	Ecole polytechnique fédérale de Lausanne
M21121	Nomenclature for a robot configuration (read from left to right, starting with the tail which is not indicated): 1 is for a body element, 2 for a leg element.
SVL	Snout-vent length
TL	Total length

Chapter 1

Introduction

The salamander, as an amphibian, is a source of inspiration for the locomotion on land and in the water and the transition between the two modes. Most species have a biphasic life cycle and develop from aquatic live as larvae towards a terrestrial live when growing up. Adult salamanders are however able to move in both environments and can overcome these natural limits. [4]

These characteristics have been used to build a robot based on the body, locomotion and behaviour of real salamanders. The robot imitates the main aspects of a salamanders gait such as the limb movement relative to the ground and the body undulation. Since the robot has a modular setup, it can be used to emulate the morphology of different species. Using different module configurations, gait parameters and walking as well as swimming mode, the robot can be tested under a widespread set of conditions. The aim of this project is to close the loop and compare again the results of this analysis with real salamanders to test if the obtained robot has indeed similar characteristics as his natural archetype.

A previous work has been done during the last semester to test the robot with different body configurations on land in the water. Since some issues occurred while comparing normalized data of robots with different total length, this work strictly focuses on the variation using a fixed body length of nine modules. The chance has been seized to extend the range of tested parameters to obtain a better basis for estimating trends on the performance and the influence of the various parameters. The available hardware has been extended for this project by a further set of limbs to test the influence of the limb size on the movement of the robot.

The results of the experimental analysis will be compared in the last part with the morphological proportions of salamanders to find a respond to the question about the analogy of the performance of the robot and the locomotor system of a salamander.

Chapter 2

Biological background

Salamanders, frogs and caecilians build the class of Amphibians. The majority of the members of this class are frogs and only 8.5% belong the order of Salamanders [7]. Most of them have a biphasic live cycle and are able to live in the water and on land.

2.1 Biodiversity

Salamanders can be found in many different habitats all over the world. They can live in tropical regions as well as in the Siberian tundra and on sea level as well as in alpine regions. Most of the salamanders grow up in an aquatic larval stage and transform to (semi-) terrestrial being animals. However, there are also species being completely terrestrial and others they remain completely aquatic. In contrast to other vertebrates, amphibians are the only type that can exploit temporary pools, puddles and water with very flat and volatile level. [4]

Family	Habitat
Cryptobranchidae	Totally aquatic in streams and rivers
Hynobiidae	Totally aquatic in streams and rivers
Ambystomatidae	Most breed in water with terrestrial adults
Amphiumidae	Totally aquatic with much reduced limbs
Dicamptodontidae	Large salamanders, breed in water with terrestrial adults
Plethodontidae	Varied group of aquatic and terrestrial forms
Proteidae	Totally aquatic
Salamandridae	Most have aquatic and terrestrial phases
Sirenidae	Totally aquatic, hindlimbs absent, forelimbs reduced

Table 2.1: Classification of the order Caudata [4, 6]

The order of Caudata is divided into nine families. They have mostly four limbs to carry their weight when emerging the water environment. The majority of salamanders has a tail that is in the order of the length of the body. The back legs are similar or slightly bigger in size as the front limbs. Some aquatic species have degenerated limbs and resemble an eel-like animal more than a salamander since they are not dependent on strong legs for the locomotion and the support of their weight [4]. The figure 2.2 illustrates the diversity of salamanders representing different families.

2.2 Locomotion

Salamanders use their entire body for the locomotion. During locomotion on land, the body is flexed from side to side and the legs push the body forwards. They use a trotting gait, meaning that the fore footfall follows the hind completely out of phase which provides the best stability during walking [5]. In addition, salamanders normally walk – in contrast to running – since the feet touch the ground at least during 50% of a gait cycle. In water, rapid movement is achieved by undulating the body while holding the limbs in a rear position near the body to minimize the resistance. The shape of the tail of a species gives therefore some indication about the efficiency of the locomotion in water. Aquatic salamanders have more flattened tails to provide more forward thrust in contrast to the more rounded tail of terrestrial salamanders. [4]

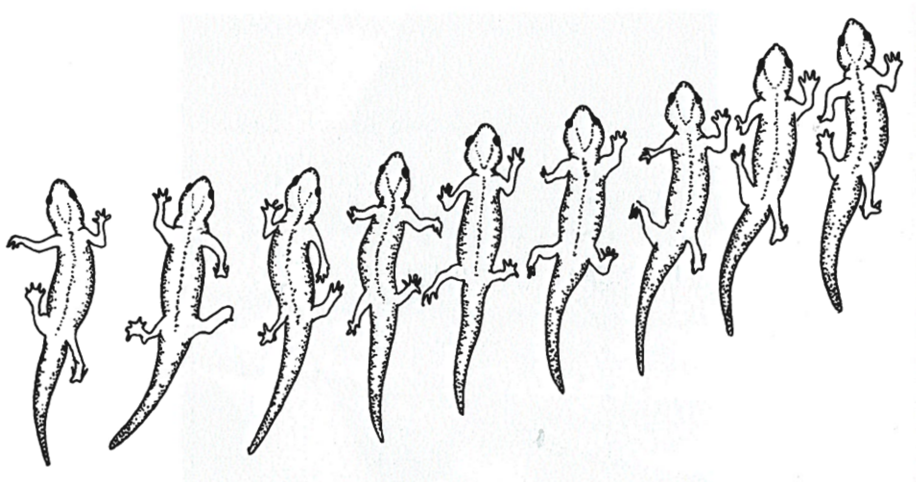

Figure 2.1: Locomotion of a salamander on land. *Redrawn from Schaeffer. S. Elmhurst [4]*

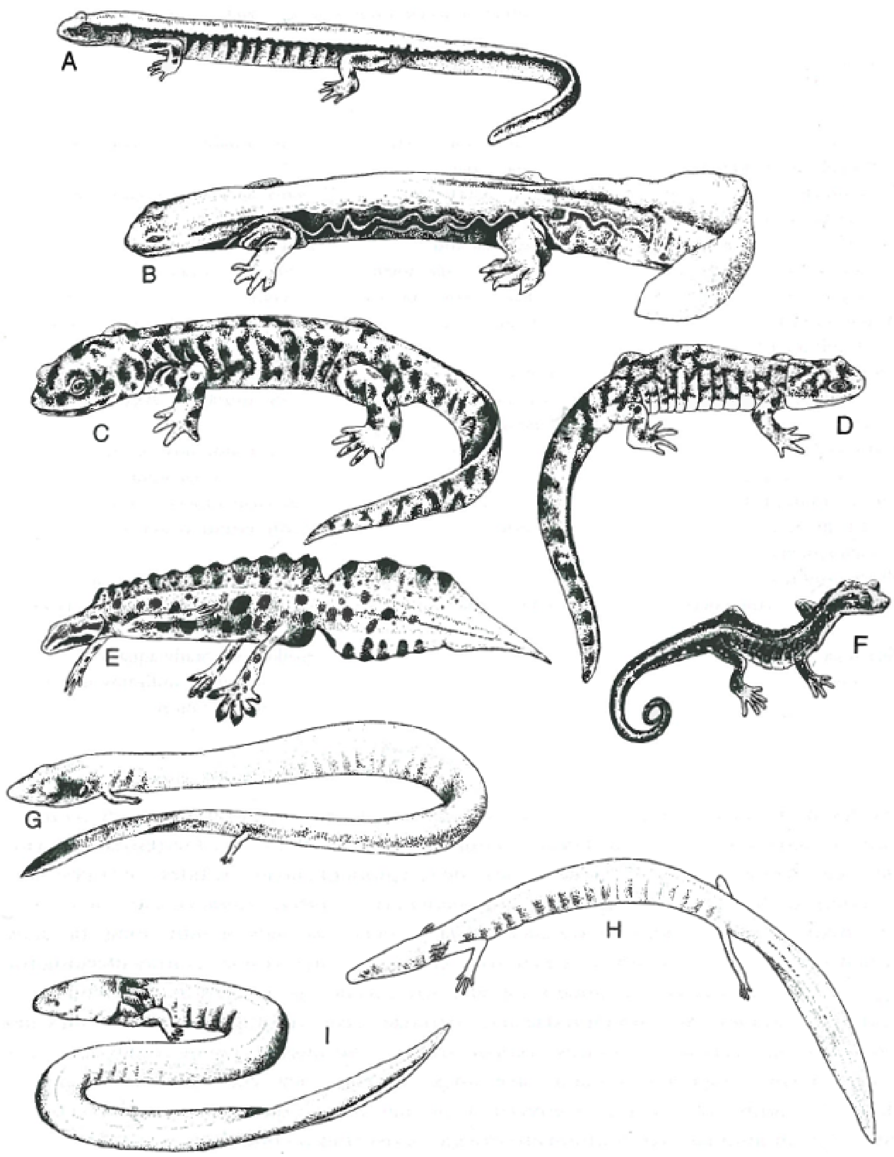

Legend: A, Hynobiidae (Salamandrella keyserlingii); B, Cryptobranchidae (Cryptobranchus alleganiensis); C, Dicamptodontidae (Dicamptodon enastus); D, Ambystomatidae (Ambystoma tigrinum); E, Salamandridae (Triturus vulgaris); F, Plethodontidae (Eurycea lucifuga); G, Amphiumidae (Amphiuma means); H, Proteidae (Proteus anguinus); I, Sirenidae (Siren lacertina). Source: P. Benson, [4].

Figure 2.2: Diversity of salamanders.

Chapter 3

Experiments

The main part of this project is the experimental analysis of the behaviour of the salamander robot. Different gait parameters and morphologies have been tested to find the best combinations for the robot for walking and swimming.

3.1 Robot

The robot used for this project is a simplified model of the locomotor system of a salamander. It is a modular system that makes it possible to emulate various morphological variations. The hardware consists of three types of modules which can be assembled to several configurations:

Head The head contains the main controller and manages the communication with the user interface. The current set points for the acutators are sent via a CAN-bus to the connected elements.

Body element The normal body elements contain a motor to manipulate the joint angle to the anterior element.

Limb element The limb element is a extended body element including two turning legs which can be controlled independently with their own motor. The limbs are exchangeable so it is possible to use legs of different size.

Every element has its own battery to provide an independent power supply during the operation. On the top of each element is one or two bright LEDs to indicate the state of a module and allow it to be detected using the tracking system of the test track. The robot can be sealed and used in the water for aquatic experiments. Without any support, it sinks to the ground of the pool but there is the possibility to add two polystyrene caps to make it swim below the water surface.

A salamander-like configuration always contains a head element followed by a limb element, a trunk part with one or several body elements, a rear limb element and several body elements for the tail. The last tail element can be complemented by a flat and stiff fin to improve the performance in the water. Several independent actuators allow to reproduce the main movements of a salamander: the undulation along the spinal column with the joint actuators and the strides of the legs with a simple rotation.

Figure 3.1: Salamander robot of the Biorobotics Laboratory.

For every experiment, a configuration with nine elements in total has been used. With the additional fin (with the same length than one robot element), the total length of the robot measures 94 cm. An additional set of limbs has been produced for this project to test the robot with longer and shorter limbs. They measure 6.75 cm and 9.25 cm respectively (distance from the center line of the robot to the ground touching point).

3.2 Parameter space

Parameters for the gait control as well as different hardware setups have been tested. Different parameter sets for the swimming and walking gaits have been used according to the behaviour of real salamanders. In contrast to the previous project, every robot configuration used the same number of elements and has therefore the same total length to improve the comparability amongst the results.

3.2.1 Terrestrial locomotion

Salamanders on the land use a simple standing wave to control the flexion of their body while trotting which leads to a curved shape along their body with fixed nodes at the pectoral and pelvic girdles [3]. When the trunk between forelimb and hindlimb is maximally displaced to one side, the head and the tail are displaced in the opposite direction. The step size of a gait is mainly governed by the length of a leg and its angle towards the center line (influenced by the body bending) which helps to increase length of the stride. Synchronous to the body bending, the limbs are oscillating with the same frequency. In a trotting gait, the movement of each pair of limbs (front and rear, diagonal) is evenly spaced in time since salamanders use symmetrical gaits [5].

The shape of the robot has to approximate the smoother shape of a real salamander with nine straight body elements and an adjustable actuator in between. A simple sinusoidal wave is used to generate the angles of the eight joints:

$$\alpha_i = A_i \sin(2\pi f t + \phi^i_{lag}) + \psi^i_{offset} \quad \forall \quad i = \{1 \dots 8\} \tag{3.1}$$

with the angle α_i of the joint i, the maximal amplitude A_i, the frequency f, phase lag ϕ^i_{lag} (which is zero for the terrestrial walking) and an additional angular offset ψ^i_{offset}. The offset ψ is only used to shift the mean angle to implement curved trajectories. It is controlled by an independent controller to keep the robot on a straight path. With exception of the phase lag ϕ, the same

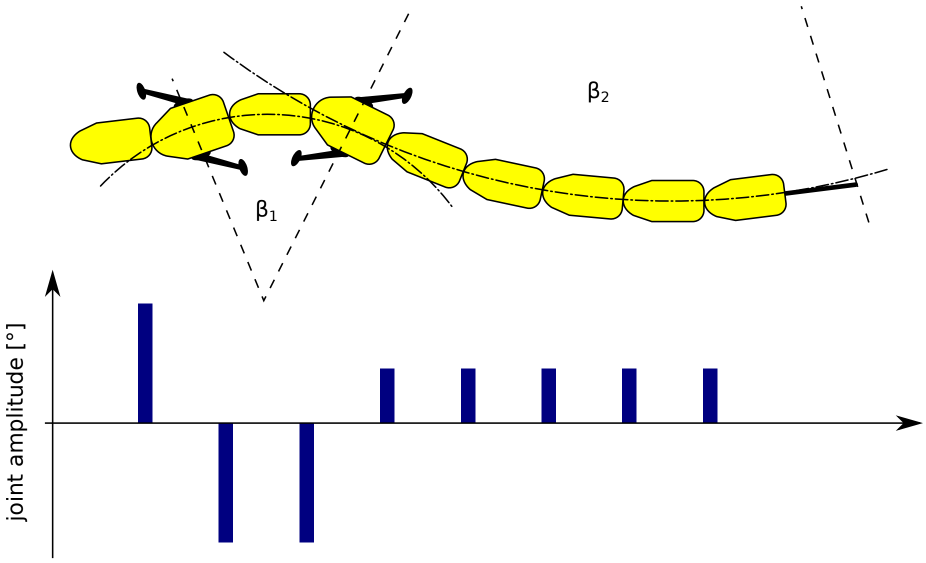

To obtain the same angle between the legs β_1, the amplitude between the head and the rear limb element is adapted to the configuration using the relation $A_{front} = \frac{\beta_1}{N}$ with the number of joints between the limb elements N ($N = 2$ for the sketched example). To obtain a natural shape of the robot, the amplitudes of the rear part are adapted according to the body proportions: $A_{rear} = A_{front}\frac{L_{front}}{L_{rear}}$ with the length L_{front} between the limb elements and the length L_{rear} of the tail.

Figure 3.2: Determination of the joint amplitude A_i.

parameters are used for every joint controller. Although salamanders can use an increasing amplitude towards the tail, for the sake of simplicity only a flat profile for A_i is used for these experiments. To obtain comparable results in terms of the length of the stride, the maximal amplitude was adapted to the used robot configuration as illustrated in the figure 3.2 to get the same bending angle β_1 between the legs for all configurations. A constant value for A_i has been used in the front part between the head and the rear leg element and an adapted value for the rear part after the second leg element to get a natural shape for every configuration.

The rotation of the legs is controlled by the duty factor which defines the duration a leg touches the ground within one cycle. If the duty factor (DF) is 50%, two feet touches the ground at any time of the gait cycle. Higher duty factors introduce overlapping periods, where both pairs of limbs touches the ground simultaneously whereas gaits with lower duty factors have periods with no ground contact at all. DF's of 50% or higher are used for the terrestrial gaits since these gaits are classified as *trotting* and correspond to a salamanders behaviour [5].

3.2.2 Swimming

During swimming, salamanders exhibit traveling waves of axial flexion and muscle activity where the wave travels from the head towards the trunk [3]. They don't use their limbs for the locomotion and keep them still in a horizontal rear position along the body. This behaviour is emulated with the same sine controller as used for the terrestrial gaits (equation 3.1) but with the addition of using a phase lag ϕ. The phase lag ϕ is related to the number of waves k along the robot by $\phi = k\frac{2\pi}{N}$ with the number of robot elements N. The four limb motors aren't actuated during the swimming phase. Only the long limbs are used for swimming because this model provides the opportunity to get retract towards the body. The lack of a second set of limbs to compare the difference for the swimming mode is not so important for this project because the position of the limbs is more in the focus of interest. Since the limbs are unused while swimming anyway, they are mainly considered as a handicap which becomes more important with increasing size. The impact of the position is however more ambiguous and is therefore part of this study.

	walking	swimming
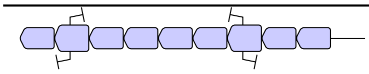	✓	✓
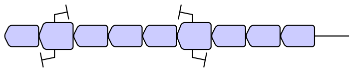	✓	✓
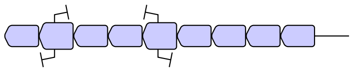	✓	✓
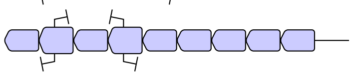	✓	✓
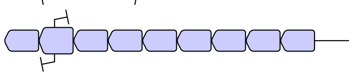	×	✓
long limbs	✓	✓
short limbs	✓	×
frequency f [Hz]	$\{0.3, 0.6, 0.9\}$	$\{0.6, 0.9, 1.2\}$
bending β_1 [°]	$\{40, 60, 80\}$	—
amplitude A [°]	—	$\{10, 20, 30\}$
duty factor	$\{50\%, 60\%, 70\%\}$	—
number of waves k	—	$\{0.25, 0.5, 0.75\}$

Table 3.1: Hardware setup and gait parameters for terrestrial and aquatic experiments.

3.3 Test procedure

The Biorobotics Laboratory is equipped with a test track of about 5 m length to test the performance of the robot. A flat pool at the ground with depth of water of about 20 cm can be used for the swimming experiments or for walking experiments when covered with wooden plates. Two overhead cameras build a tracking system to localize the position of bright LEDs and store a log file for every experiment for a later analysis. A previous calibration allows to get absolute coordinates about the positions of the detected light sources. A further top mounted camera allows to capture video clips of an experiment for a visual inspection.

The combination of the selected values for each varied parameter leads quickly to a big amount of test cases. For the benefit of a wide range of parameters, each setting has been tested only once in contrast to the prior semester project where an experiment has been repeated three times. It allowed to survey one more robot configuration and a second set of limbs in comparison with the last semesters project. This reduction of data per test case was compensated by a more accurate analysis of each experiment. Instead of using the averaged speed measurements of an entire run, the data has been split up and analysed in three different intervals independently. The selection of three parts for the analysis of each run had to be done by hand to ensure to analyse undisturbed and error free data sets.

3.3.1 Walking experiments

Almost two-thirds of the experiments have been performed on land because of the two sets of limbs which increased the amount of parameter combinations compared to the swimming part. Every run has been captured by the tracking system and the overhead video camera. The speed of the robot was calculated using the center of mass of the robot traveling along the line of locomotion. Three parts of the tracking data containing at least one entire gait cycle have been analysed separately for each experiment to obtain a sufficiently robust result.

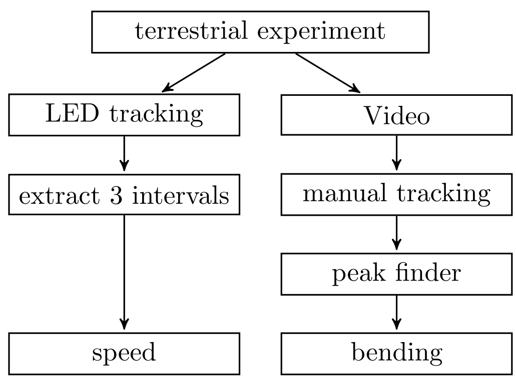

Figure 3.3: Work flow for the terrestrial experiments.

A big issue of the previous work was the uncertainty about the actual used bending angle of the robot during the run. There was obviously a discrepancy

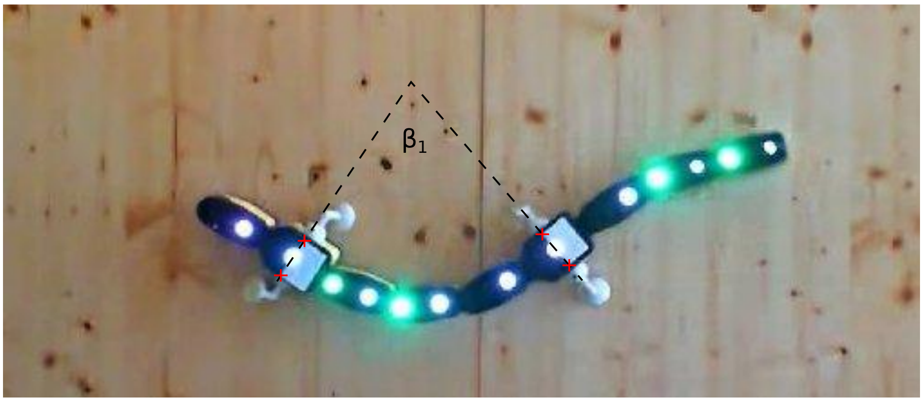

Four points of the limb elements are tracked (illustrated with four red crosses in the image) throughout the video data of a walking experiment. The peaks the obtained bending curve $\beta(t)$ represent the real bending angle of a gait.

Figure 3.4: Video tracking for the determination of the axial flexion during a walking gait.

between the set point of the sine controller and the effected angle because of backlash and torque restrictions in every joint. For this reason, the bending has been measured for every experiment to get a more realistic view of the results (see fig. 3.4). At least three gait cycles have been analysed for every run. The mean value of the amplitude of the flexion to the left side and to the right side helps to eliminate the effect of the additional offset to keep the salamander on a straight line assuming that this value doesn't change a lot within a gait cycle.

3.3.2 Swimming experiments

A similar approach has been used for the aquatic experiments. The same issues as mentioned in the previous section also apply for the swimming gaits: the real amplitude is not known since there are significant differences expected. In contrast to the terrestrial runs, it was simpler to determine the real amplitude because this information can be extracted out of the tracked coordinates of the LEDs and no manual video tracking is needed for this part.

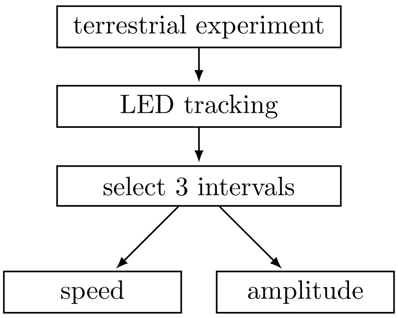

Figure 3.5: Work flow for the aquatic experiments.

Chapter 4

Results

This chapter summarizes all results obtained from the experiments of this projects. The data for the terrestrial and aquatic part is presented in two separate sections because they can't be compared directly among each other. A detailed overview of the performance of each run is presented in the appendix A.

4.1 Walking robot

Every run leads to a measured speed (as an average of three values) as function of the used module configuration, limb size, gait frequency, amplitude and duty factor. While the morphology is a fixed hardware setting, the gait parameters are continuous variables. The gait frequency and the duty factor meet the setpoint within a close range whereas the amplitude varies strongly depending on the morphology and the frequency. This behaviour made it difficult to reach an overlapping range for the tested amplitudes since the amplitude decreases with higher frequency and some torque restrictions appeared. The effort to reach a desired axial flexion between the limb elements is divided by the number of joint actuators according to the robot configuration. The torque limits are therefore reached at a lower axial flexion for morphologies with shorter limb distance. Further limits for the amplitude occurred for the configurations with only one element between the limbs because it has to be avoided that the feet touch each other during the walk.

A view on the raw results can already identify some main trends about the influence of the tested parameters on the robots performance:

- The *gait frequency* has an important impact on the speed of the robot. Three groups for the frequency values $f = \{0.3\,\text{Hz}, 0.6\,\text{Hz}, 0.9\,\text{Hz}\}$ can be separated clearly – a higher frequency leads to a faster movement.
- A higher *amplitude* leads to a faster locomotion, although the performance is less sensitive to this parameter.
- The *duty factor* only plays a secondary role regarding the speed of the robot. The trend shows, that the speed decreases slightly if the limbs touch the ground longer.

The eight morphologies have to be compared under the same conditions. For this reason, the speed results have been interpolated and compared for a bending β_1 of 60 ° because this is a point where every test group overlap. A quadratic interpolation has been used to determine the speed at 60 ° since there are three measured points and a second order polynomia seems to be appropriate to represent the relation between the speed and the amplitude. This data has been scanned for the fastest run of each morphology which occurred at a frequency of 0.9 Hz and a duty factor of 50 % in any case.

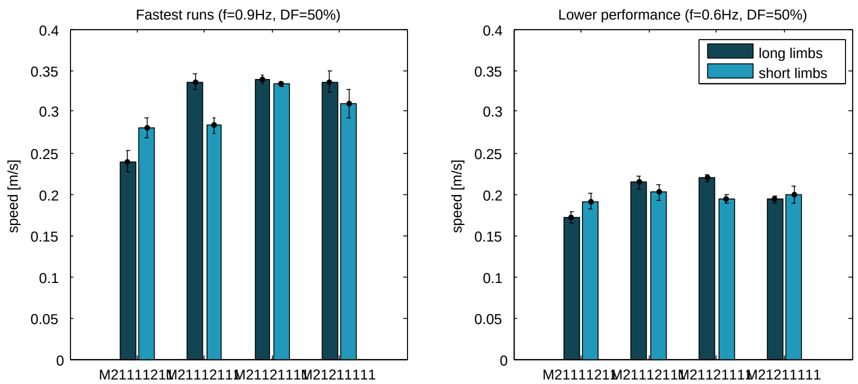

Figure 4.1: Comparison of the walking performance among the morphologies.

The comparison between the robot with long and short limbs shows a tendency that longer limbs are beneficial for the robots locomotion. Even though this observation is not valid for every parameter set, it meets the most efficient cases as it can be seen in the figure 4.1. Because of the very flat shape for the maximal speed for the robot with long limbs, the same analysis has been repeated using the next lower frequency of 0.6 Hz to check if this effect also occurs if the robot is not running at its highest speed. The main difference between these two data sets is the lower performance of the M21211111 configuration using long limbs and the more even speeds for the robot using the short limbs.

It can be seen, that the robot configuration with four elements between the limbs (M21111211) is the slowest morphology using the long limbs as well as the short limbs. The result is less clear for the best configuration. While the speed of the robot increases when the rear limbs come closer to the front limbs, there is also a decreasing effect for the other exrem case where only one element is used between the two limb elements. The optimal morphology for terrestrial walking seems to be therefore the M21121111 configuration using long limbs.

4.2 Swimming robot

The analysis of the data for the swimming experiments is similar to the part of the terrestrial walking – a speed value is obtained for every parameter combination (as an averaged value of three measurements). Although there are no strict rules of the resulting patterns, the following trends can be identified:

- A higher *frequency* leads to a faster locomotion (when leaving the other parameters) but the groups can't be distinguished as well as for the walking gaits.
- The *amplitude* has an important impact on the speed of the robot which is strictly increasing but with varying slope. The advantage of a higher amplitude becomes more important in combination with a high frequency.
- The influence of the *number of waves* is less evident. The lowest value of $k = 0.25$ is in most of the cases clearly slower than the other two tested values $k = 0.5$ and $k = 0.75$. It can't be evaluated which of these two values is decidedly the best one since the results are close and overlap within a standard deviation in many cases.

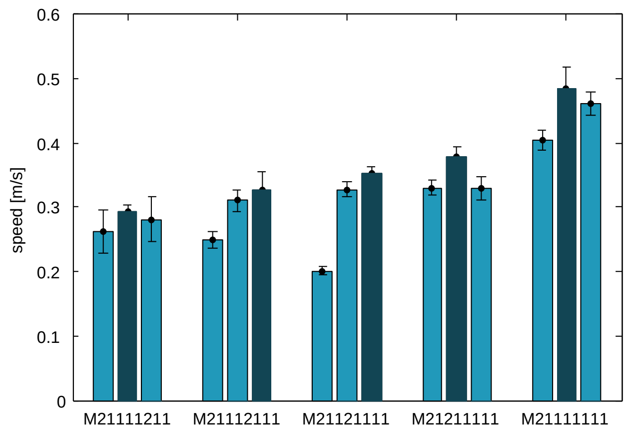

Three results per morphology for the runs at a frequency of $f = 1.2$ Hz and an amplitude of $A = 20$ are presented in this figure. The bar on the left side represents a number of waves $k = 0.25$, the middle bar is for $k = 0.5$ and the right hand bar for $k = 0.75$. A dark bar indicates the fastest run for a morphology.

Figure 4.2: Comparison of the swimming performance among the morphologies for a joint amplitude of 20 degrees.

For a further comparison of the results among the morphologies, the speed curves have been interpolated using a second order polynomial and evaluated for a joint amplitude of 20 degrees. The figure 4.2 summarizes the speed results for the runs at the highest frequency of 1.2 Hz and all three tested values for the number of waves to demonstrate the impact of this value. An important trend in this data is the slightly better performance for a morphology with a smaller distance between the limb elements. The most efficient morphology is the sirene-like configuration with only one limb element as it can be expected regarding the resistance caused by the limbs.

Chapter 5

Robot in comparison with salamanders

After the exploration of a wide range of experiments, the best suited hardware configuration has been selected regarding the speed of the robot. This chapter compares these results with the morphologies of real salamanders to check, if the simple locomoter system has a similar behaviour than real salamanders. It is assumed that the evolutionary development led to an optimal morphology for every species. The optimal shape of the body of an animal is not only the best solution in terms of reaching the highest speed since there are further important influences like the efficiency of a gait, the concrete environment (e.g. forest, wetland, grassland), respiration, temperature regulation, feeding, defence and others. However, the ability of a fast movement is considered to be important for an animal in the nature and has an important impact on the development of the morphology.

5.1 Robot morphology

The previous chapter compared the obtained speed of the robot using different hardware settings. The experiments can identify a favorable configuration for the tested circumstances – for walking on a flat ground and swimming. Similar trends of the effect of a variation of a parameter allow to make a supposition for a robot capable to operate in both modes, walking and swimming. The extreme case for swimming with only one limb element does not come into consideration for an amphibian application because it is not appropriate to move on land. The limb size has an opposing effect on the speed of the robot for swimming and walking: while the results are better with bigger limbs on land, they only cause more friction while swimming – this can be observed comparing the swimming experiments with one and two limb modules. A trade-off between these two effects would be a robot with the short limbs since they don't decelerate the walking robot too much (see fig. 4.1) with the condition that the limbs can be folded towards the body.

5.2 Salamander morphology

As illustrated in the chapter 2, salamanders can have a wide spread of different morphologies. Only species found in Europe are considered in this project as basis of comparison to set some limits on the amount of biological data. The measurements have been extracted by hand out of photographs because there was no comprehensive database of morphological data. This approach is not very precise because of measurement errors and a natural variability of the salamanders. In spite of this issues, the histogram presented in the figure 5.1 shows a clear trend. The measured index represents the ration of the body length (distance from the head to the rear limbs) to the total length of the salamander. This value is close to the commonly used SVL/TL ratio but it can be measured easier using photographs. The variation of the body-tail ratio is in a very close range where the tail has equal length or is slightly longer than the body length. For the aquatic salamanders, the case is less evident because there are only five entirely aquatic species found in Europe. There is however the same trend for a body/TL ratio around 0.5. The used values for this analysis are listed in a table in the appendix B.

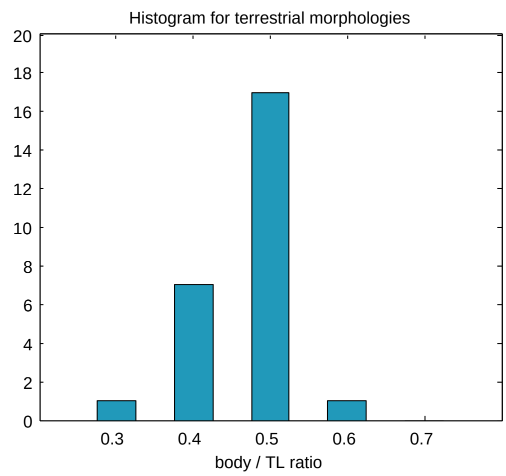

Figure 5.1: Histogram of the body/TL ratio of terrestrial living salamander species find in Europe.

The results about the length of the limbs are more difficult to compare. No accurate data is available about these proportions and it is difficult to measure them only using photographs. There exists for this purpose the *Wolterstorff Index* (WI) which is used in the literature as an indicator for taxon identification and is defined by the ratio between the forelimb length and the interlimb distance [1]. Unfortunately, only few concrete values can be found in the literature. This index is mainly used to distinguish Crested Newts and is well known for these four families. It lies normally in a range between 0.1 for salamanders with short legs [2] and about 0.6 for salamanders with long and strong legs [4].

5.3 Comparison

The same indices used for the salamander morphologies have been calculated for the robot configurations. The range of the tested body to TL ratios is within 0.4 and 0.7 and fits to the observed values in nature. Furthermore, the selected configuration for the terrestrial and amphibian application (M21121111) with a body/TL ratio of 0.5 lies in the same region as most of the inspected salamander species. The result for the swimming robot to prefer a configuration with only two limbs can also be approved regarding the various species with degenerated limbs if they don't use them on land or for underwater stepping.

Robot configuration	body/TL	WI short limbs	WI long limbs
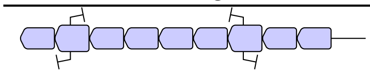	0.7	0.09	0.14
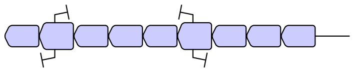	0.6	0.11	0.17
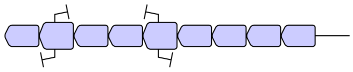	0.5	0.14	0.23
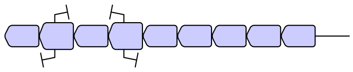	0.4	0.21	0.35

Table 5.1: Body/TL ratio and Wolterstorff Index for the used robot configurations

The limb proportions are more difficult to compare because of physical differences. Since the robot has no real feet and digits, no accurate results can be expected when comparing the length of the legs between the robot and salamanders. For this reason it has to be kept in mind, that the robot tends to have a lower WI compared to real salamanders. The selected configuration for terrestrial walking (M21121111 with long limbs) with a WI of 0.23 doesn't reach the same value for the WI compared to a Crested Newt with chunky limbs with a WI of up to 0.6 which marks however the upper bound found in nature. The results are closer regarding the aquatic case: the swimming robot with a WI of 0.14 is in the same range as the also aquatic Blind Cave Salamander with a WI within $0.11 - 0.16$ [2].

Chapter 6

Conclusion

The salamander robot of the Biorobotics Laboratory has been tested with a wide spread of parameters and different hardware settings. These experiments led to a data set where the influence and the trend of each varied value can be analyzed. A big issue of the previous work – the unknown difference between the desired joint amplitude and the real value – could be eliminated with the tracking and measuring of the data of each experiment. The prize of this advantage is the reduction of the repetitions to only one run per parameter set which leads to a more ambiguous result.

The evaluation and interpretation of the obtained results lead to the fastest robot setup for terrestrial walking and swimming. A combination of these trends is used for an estimation about the fastest configuration for an amphibian operation of the robot. The case of underwater stepping has however not be taken into account since it was not in the range of this work.

Operation mode	Robot configuration
Walking on land	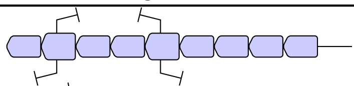
Swimming	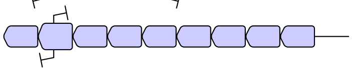
Walking and swimming	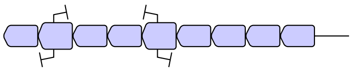

Table 6.1: Selected robot configurations for different environmental requirement.

Assuming, that the natural development already optimized the morphology of salamanders, they are compared with the best suited configuration for the robot. Although an optimization of the body shape doesn't mean for a real animal to select the fastest one, the ability to move fast is considered to be an important driving force in the evolutionary process. There is however no doubt that other aspects like the efficiency, the specific environment, temperature regulation, defense strategy, feeding and many more also influence the development. This can explain the big variations of morphologies within the family of salamanders. In spite of many differences, a rough analysis of the main body proportions showed a relatively homogeneous pattern. Most of the species found in Europe have equal or slightly shorter body than the tail length.

The observed trends about the morphology of salamanders is in good coincidence with the same characteristics of the selected robot configurations obtained by the experimental optimization. This result allows to state a similar behaviour of the locomotor system of a salamander and the robot. Although the robot emulates the salamanders locomotion in a very simplified manner, it underlies the same trends as real salamanders. It demonstrates a successfully realization of the robot design inspired by the salamanders.

Appendix A

Measurements

The results of all experiments are visualized on the next two pages. Each value in the plots consists of the mean value of three measurements in the tracked data of one run.

A.1 Terrestrial walking with short limbs

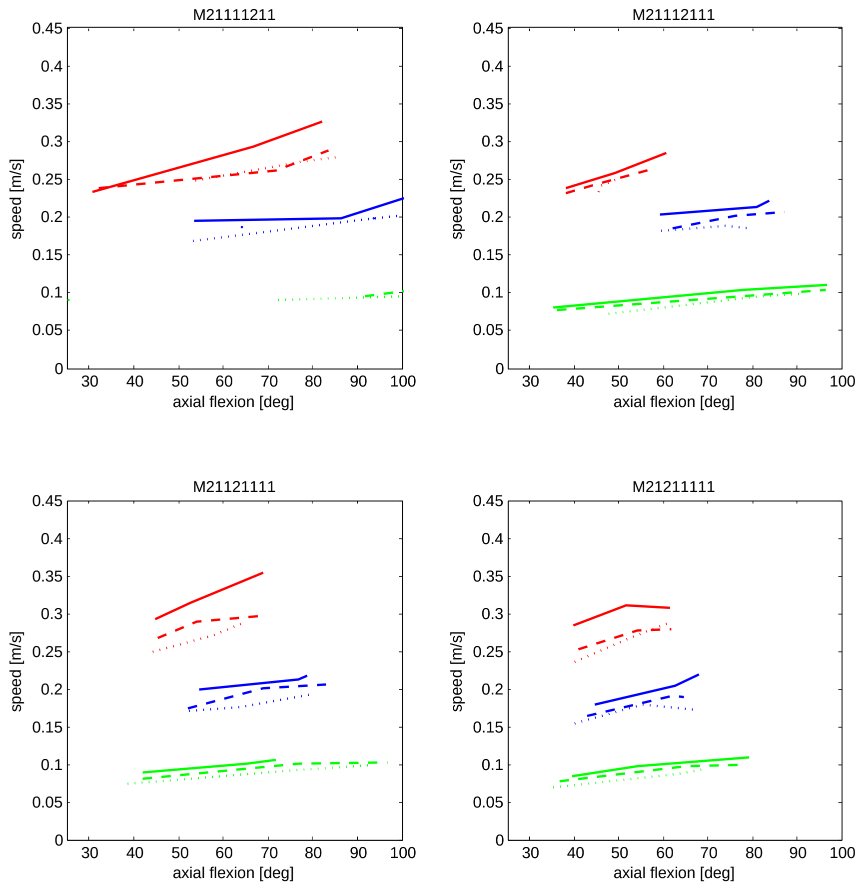

Legend: green: $f = 0.3\,\text{Hz}$; blue: $f = 0.6\,\text{Hz}$; red: $f = 0.9\,\text{Hz}$; solid: $DF = 50\%$; dashed: $DF = 60\%$; dotted: $DF = 70\%$;

Figure A.1: Data overview for walking robot with short limbs.

A.2 Terrestrial walking with long limbs

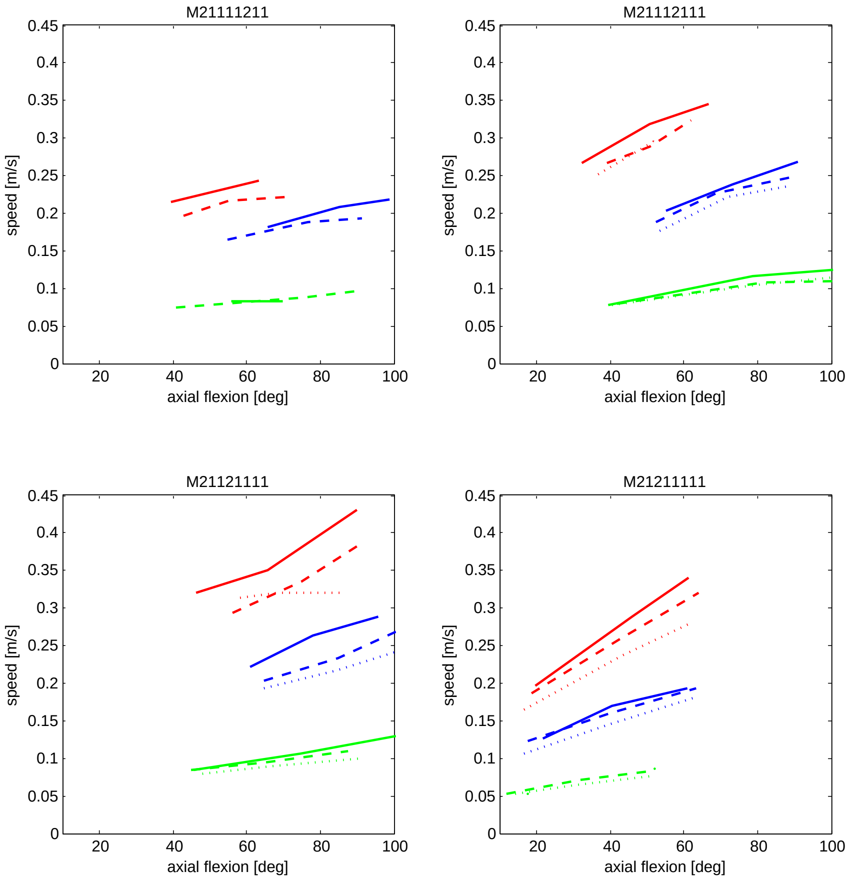

Legend: green: $f = 0.3\,\text{Hz}$; blue: $f = 0.6\,\text{Hz}$; red: $f = 0.9\,\text{Hz}$; solid: $DF = 50\%$; dashed: $DF = 60\%$; dotted: $DF = 70\%$;

Figure A.2: Data overview for walking robot with long limbs.

A.3 Swimming

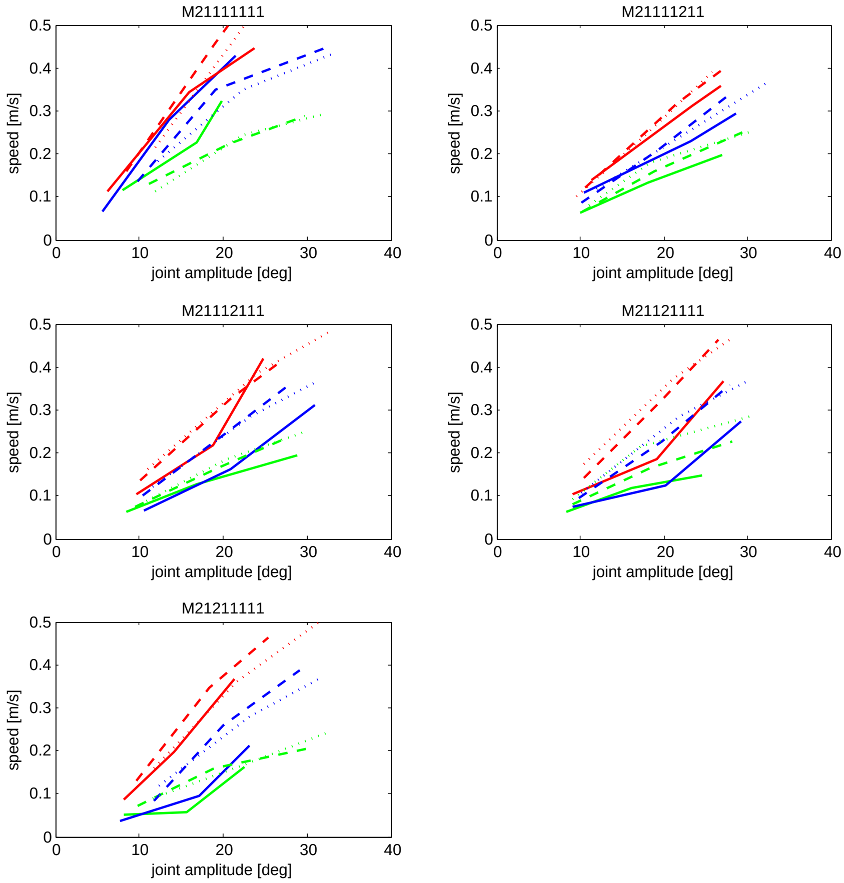

Legend: green: $f = 0.3\,\mathrm{Hz}$; blue: $f = 0.6\,\mathrm{Hz}$; red: $f = 0.9\,\mathrm{Hz}$; solid: $k = 0.25$; dashed: $k = 0.5$; dotted: $k = 0.75$;

Figure A.3: Data overview for swimming.

Appendix B

Morphologies of European salamanders

family	species		habitat	body/TL ratio
Plethodontidae	Hydromantes ambrosii	Spezia Cave Salamander	te	0.5
	Hydromantes strinatii	North-west Italian Cave Salamander	te	0.5
	Hydromantes italicus	Italian Cave Salamander	te	0.5
	Hydromantes genei	Sardinian Cave Salamander	te	0.5
	Hydromantes imperialis	South-east Sardinian Cave Salamander	te	0.6
	Hydromantes supramontis	Supramonte Cave Salamander	te	0.5
	Hydromantes flavus	Monte Albo Cave Salamander	te	0.5
Salamandridae	Triturus boscai	Bosca's Newt	aq	0.4
	Triturus helveticus	Palmate Newt	aq	0.5
	Triturus italicus	Italian Newt	aq	0.5
	Triturus montandoni	Carpathian Newt	te	0.5
	Triturus vulgaris	Smooth or Common Newt	te	0.5
	Triturus alpestris	Alpine Newt	te	0.5
	Triturus vittatus	Banded Newt	te	0.4
	Triturus carnifex	Alpine Crested Newt	te	0.5
	Triturus cristatus	Northern Crested Newt	te	0.5
	Triturus dobrogicus	Danube Crested Newt	te	0.5
	Triturus karelinii	Southern Crested Newt	te	0.5
	Triturus marmoratus	Marbled Newt	te	0.4
	Euproctus asper	Pyrenean Brook Salamander	se	0.5
	Euproctus montanus	Corsican Brook Salamander	te	0.4
	Euproctus platycephalus	Sardinian Brook Salamander	te	0.4
	Pleurodeles waltl	Spanish Ribbed Salamander	aq	0.5
	Salamandrina terdigitata	Spectacled Salamander	te	0.4
	Salamdra atra	Alpine Salamander	te	0.5
	Salamandra lanzai	Lanza's Alpine Salamander	te	0.5
	Salamandra salamandra	Fire or Spotted Salamander	te	0.5
	Mertensiella caucasica	Caucasian Salamander	te	0.4
	Mertensiella luschani	Luschan's Salamander	te	0.4
	Chioglossa lusitanica	Golden-striped Salamander	te	0.3
Proteidae	Proteus anguinus	Blind Cave Salamander	aq	0.7

Legend: te: terrestrial salamander (regardless of the breeding season), aq: aquatic salamander, se: (semi-) terrestrial salamander, remains in the water in some regions

Figure B.1: Body/TL ratio for species found in Europe. Data sources: [4], photographs used from `http://www.caudata.org`

Bibliography

[1] J. W. Arntzen and Graham P. Wallis. Geographic variation and taxonomy of crested newts (triturus cristatus superspecies): morphological and mitochondrial dna data. *Contributions to Zoology*, 68(3), 1999.

[2] J.W. Arntzen and B. Sket. Speak of the devil: the taxonomic status of proteus anguinus parkelj revisited (caudata: Proteidae). *Herpetozoa*, 8(3/4):165–166, 1996.

[3] Larry M. Frolich and Andrew A. Biewener. Kinematic and electromyographic analysis of the functional role of the body axis during terrestrial and aquatic locomotion in the salamander ambystoma tigrinum. *Journal of Experimental Biology*, 162(1):107–130, 1992.

[4] Richard A. Griffiths. *Newts and Salamanders of Europe.* Poyser Natural History, 1996.

[5] Milton Hildebrand. The quadrupedal gaits of vertebrates. *BioScience*, 39(11):pp. 766–775, 1989.

[6] Roy W. McDiarmid and W. Ronald Heyer. *Measuring and Monitoring Biological Diversity: Standard Methods for Amphibians.*, chapter Amphibian Diversity and Natural History: An Overview. Smithsonian Institution Press, 1994.

[7] James W. Petranka. *Salamanders of the United States and Canada*. Smithsonian Institution Press, 1998.